Heliyon 10 (2024) e37137

Contents lists available at ScienceDirect

Heliyon

journal homepage: www.cell.com/heliyon

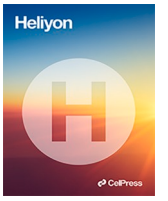

Research article

The S341P mutant MYOC renders the trabecular meshwork sensitive to cyclic mechanical stretch

Xuejing Yan [a,b], Shen Wu [a,b], Qian Liu [a,b], Yufei Teng [a], Ningli Wang [a,b], Jingxue Zhang [a,b,*]

[a] *Beijing Institute of Ophthalmology, Beijing Tongren Eye Center, Beijing Tongren Hospital, Capital Medical University, Beijing Ophthalmology & Visual Sciences Key Laboratory, Beijing, 100730, China*
[b] *Beijing Institute of Brain Disorders, Collaborative Innovation Center for Brain Disorders, Capital Medical University, Beijing, 100069, China*

ARTICLE INFO

Keywords:
Glaucoma
Trabecular meshwork
MYOC
Mechanical stretch

ABSTRACT

The trabecular meshwork (TM) plays an essential role in the circulation of aqueous humor by sensing mechanical stretch. The balance between the outflow and inflow of aqueous humor is critical in regulating intraocular pressure (IOP). A dysfunctional TM leads to resistance to the outflow of aqueous humor, resulting in an elevated IOP, a major risk factor for glaucoma. It is widely accepted that mutant myocilin (MYOC) can cause damage to the TM. However, few studies have investigated how TM cells carrying mutant MYOC respond to cyclic mechanical stretch (CMS) and whether these cells are more sensitive to CMS under this genetic background. In this study, we applied mechanical stretch to TM cells using the Flexcell system to mimic physiological stress. In addition, we performed genome-wide transcriptome analysis and oxidized lipidomics to systematically compare the gene expression and oxylipin profiles of non-stretched control human primary TM cells, human primary TM cells under CMS (TM-CMS), and human primary TM cells overexpressing $MYOC^{S341P}$ under CMS (S341P-CMS). We found that TM cells that overexpressed $MYOC^{S341P}$ were more sensitive to mechanical stress. Kyoto Encyclopedia of Genes and Genomes (KEGG) analysis revealed that downregulated genes were most enriched in oxidative phosphorylation, indicating mitochondria dysfunction and the likelihood of oxidative stress. Oxidized lipidomics analysis revealed significant changes in oxylipin profiles between the S341P-CMS and TM-CMS groups. Through further genome-wide transcriptomic analysis, we identified several genes that may be involved in the sensitivity of TM cells that overexpressed $MYOC^{S341P}$ to mechanical stress, including *SARM1*, *AHNAK2*, *NT5C*, and *SOX8*. The importance of these genes was validated by quantitative real-time PCR. Collectively, our findings indicate that mitochondrial dysfunction may contribute to the damage that occurs to TM cells with a $MYOC^{S341P}$ background under mechanical stretch.

1. Introduction

Glaucoma is a leading cause of irreversible blindness and is characterized by optic nerve atrophy and visual field loss [1]. The global incidence of glaucoma is 3.54 % in individuals aged 40–80 years, and this is expected to exceed 100 million by 2040 [2]. The

* Corresponding author. Dongjiaominxiang Street, Dongcheng District, Beijing, 100730, China.
E-mail address: jingxuezh@ccmu.edu.cn (J. Zhang).

https://doi.org/10.1016/j.heliyon.2024.e37137
Received 27 March 2024; Received in revised form 27 August 2024; Accepted 28 August 2024
Available online 29 August 2024

elevation of intraocular pressure (IOP) is known to be a major risk factor for optic nerve damage in glaucoma. Aqueous humor balance is critical in maintaining IOP homeostasis. The trabecular meshwork (TM) is the main tissue responsible for regulating the circulation of aqueous humor and is also the critical site for abnormal increases in outflow resistance [3]. Dysfunction of the TM can cause an elevation in the IOP, eventually leading to glaucoma [4]. TM cells are continuously exposed to mechanical distortion due to variations in IOP. Even in a normal physiological state, the IOP does not remain constant; rather, blinking and other eye movements can cause the IOP to fluctuate by up to 10 mmHg [3]. Therefore, it can be inferred that TM cells should be capable of coping with physical stress and preventing stress-induced injury.

TM cells maintain cellular homeostasis in response to mechanical stretch via mechanosensitive channels [5], cytoskeletal remodeling [6], nitric oxide signaling [7], and autophagy [8]. The concerted action of these biological processes constitutes an adaptive mechanism by which TM cells cope with physical stress. However, in cases involving long-term pathological increases in IOP, cells can fail to maintain cellular homeostasis, thus resulting in irreversible damage to TM tissue.

MYOC was the first gene identified as causally linked to primary open-angle glaucoma [9]. Furthermore, the $MYOC^{S341P}$ mutation has been proven to be associated with severe glaucoma phenotypes in a five-generation family suffering from primary open-angle glaucoma [10]. Our research group, and others, have performed *in vitro* and *in vivo* studies that mutant MYOC can impair the TM predominantly by endoplasmic reticulum-stress-mediated autophagy deregulation [11–13]. However, researchers have yet to investigate the specific biological significance of $MYOC^{S341P}$ under mechanical stress. Furthermore, how TM cells carrying the $MYOC^{S341P}$ mutation respond to cyclic mechanical stretch (CMS) and whether they are more sensitive to mechanical stress has yet to be determined.

Oxylipins, a group of bioactive lipids derived from the oxygenation of polyunsaturated fatty acids, play a crucial role in a range of physiological and pathological processes, including inflammation, immune response, and cell death [14]. In the context of glaucoma, oxylipins have been implicated in the regulation of IOP and the survival of retinal ganglion cells. Emerging research suggests that the dysregulation of oxylipin pathways may contribute to the pathogenesis of glaucoma by promoting oxidative stress and inflammation [15]. In addition, MYOC has been linked to the oxidative stress response; mutations in MYOC have been shown to trigger endoplasmic reticulum stress and apoptosis in TM cells, potentially influenced by oxylipin-mediated signaling pathways. Understanding the specific interplay between oxylipins and MYOC mutations will provide valuable insights into the molecular mechanisms underlying glaucoma and may identify potential therapeutic targets.

In the present study, we first investigated transcriptomic and oxylipin changes in human primary TM cells expressing the $MYOC^{S341P}$ mutation in response to mechanical stretch stimuli. Then, we investigated the downstream signaling pathway in response to stretch stress in human primary TM cells with and without the $MYOC^{S341P}$ mutation.

2. Materials and methods

2.1. Cell culture

Human primary TM cells were obtained from ScienCell Corporation (Carlsbad, CA, United States, catalog: 6590) and grown in TMCM culture medium (ScienCell, catalog:6591) supplemented with 2 % fetal bovine serum (ScienCell, 0025), 1 % penicillin/streptomycin solution (ScienCell, 0503), and 1 % TM cell growth supplement (ScienCell, 6592). We used one strain of human primary TM cells from a single individual. The donor came from a 22-year-old woman. Prior to experimentation, all cells were cultured for <6 passages.

2.2. Drug treatment

A stock solution of dexamethasone (Dex. Selleck, S1322) was prepared with dimethyl sulfoxide (Beyotime, ST038), and drugs were diluted in culture medium prior to the treatment of human TM cells. TM cells were treated with Dex at a concentration of 100 nM for 7 days and then harvested for subsequent analysis.

2.3. Plasmid construction and lentivirus packaging

Plasmid construction and lentivirus packaging were performed by WZ biosciences. Briefly, coding sequence (CDS) of $MYOC^{S341P}$ were synthesized and cloned into the lentivirus vector pLenti-Puro. Subsequently, the sequences were verified by DNA sequencing. Next, the empty vector and the pLenti-$MYOC^{S341P}$ vector were co-transfected with the packaging plasmids PMD2G and PXPAX2 into human embryonic kidney 293 (HEK 293T) cells. Three days after transfection, the virus supernatants were filtered by sucrose gradient ultracentrifugation.

2.4. Lentiviral infection

Human primary TM cells were seeded into six-well plates at a density of 1.0×10^5 cells per well the day before infection and reached 50–60 % confluency the following day. Next, the cells were infected with the empty vector control or $MYOC^{S341P}$ lentivirus at a multiplicity of infection of 10; then, polybrene (MCE, HY-112735) was added to the cells at a concentration of 6 μg/ml. The culture medium was replaced with fresh medium within 24 h, and the cells were harvested for subsequent analysis at specific timepoints.

2.5. CMS

Human primary TM cells were seeded into plates that had been pre-coated with collagen I (Flexcell International Corporation, BF-3001C). Once the cells reached 90 % confluency, they were starved for 2 h. Then, the plates were placed on a Flexcell 5000 Tension System (Flexcell International Corporation, Burlington, NC), and the cells were subjected to 15 % stretching at 1 Hz for 24 h. Cells in the control group were cultured under the same conditions but were not subjected to CMS.

2.6. Cell death detection

Cell death detection kit was purchased from YEASEN (40302ES50). TM cells were digested using EDTA-free trypsin (biosharp, BL526A) for 1 min, centrifuged for 5 min at 300*g* and washed twice with pre-cooled phosphate-buffered saline (PBS). Subsequently, cells were resuspended in 1 × binding buffer at a final concentration of 2×10^6/ml. Finally, propidium iodide staining solution (10 μl) and PBS (400 μl) were added to the cells, and flow cytometry was immediately conducted to analyze cell death.

2.7. mRNA sequencing

Following CMS, cells were washed with 1 × PBS, and TRIzol reagent was added to the wells for total RNA extraction in accordance with the manufacturer's instructions. RNA samples (2 μg) were then used to prepare sequencing libraries with a NEBNext Ultra RNA Library Prep Kit for Illumina (NEB, USA), in accordance with the manufacturer's instructions. Following cluster generation, the prepared libraries were sequenced on an Illumina HiSeq 4000 platform to generate paired-end 150-base pair (bp) reads. Following quality control, high-quality reads were mapped to the reference genome sequence. Only reads with a perfect match, or a single base-pair mismatch, were further analyzed and annotated in comparison with the reference genome.

Differential expression analysis was performed using the DESeq package in R (version 1.10.1). The resulting P-values were adjusted by the Benjamini and Hochberg approach to control the false discovery rate. Genes with an adjusted $P < 0.05$ according to DESeq were defined as being differentially expressed genes (DEGs). Functional and Kyoto Encyclopedia of Genes and Genomes (KEGG) pathway analyses of the annotated DEGs were conducted using the GOseq R package and KOBAS software.

2.8. Oxylipin extraction, lipid chromatography, and mass spectrometry

These analyses were performed by Wuhan Metware Biotechnology Co., Ltd. (Wuhan, China). In brief, the cell samples were harvested and oxylipins were extracted according to the manufacturer's instructions. Ultra-high-performance liquid chromatography with tandem mass spectrometry was then used for oxylipin analysis. Resultant data were analyzed with reference to the Metware database, and cluster analysis was performed for differential oxylipin content.

2.9. Quantitative real-time polymerase chain reaction (qRT-PCR) analysis

Cells were harvested and total RNA was extracted with TRIzol reagent (Thermo, 15596026CN) in accordance with the manufacturer's instructions. Next, 500 ng of total RNA was reverse transcribed into cDNA with HiScriptII Q RT SuperMix for qPCR (Vazyme, R223-01). qRT-PCR was then performed with ChamQ TM Universal SYBR qPCR Master Mix (Vazyme, Q711-02) on a Bio-Rad machine (Hercules, CA). The primer sequences were as follows: Sarm1 sense, 5′- TGCTCGACTCTAACCGCTTGGA -3′ and antisense, 5′-TCGCTGAACACCTTGGTCTTGC-3′; AHNAK2 sense, 5′-AGGTCTCGGTGGATGTGTCTGC-3′ and antisense, 5′- TGCGGAGGT-CAGTGGTCTTGAG-3′; NT5C sense, 5′- CGGACACGCAGGTCTTCATCTG -3′ and antisense 5′-CGATTGTGGCAGCAGGTGAACA-3′; SOX8 sense, 5′- CTTGCTGAGCGAGAGCGAGAAG -3′ and antisense, 5′-GCCGTGGCTGGTACTTGTAGTC-3′; β-actin sense, 5′-CATG-TACGTTGCTATCCAGGC-3′ and antisense, 5′- CTCCTTAATGTCACGCACGAT -3′. β-actin served as the internal control.

2.10. Western blot analysis

TM cells were lysed in RIPA buffer (Beyotime, P0013B) for 30 min on ice. Protein concentrations were then quantified with a BCA kit (Thermo, 23227). Total protein aliquots (40 μg) were then subjected to 10 % sodium dodecyl sulfate-polyacrylamide gel electrophoresis and transferred to polyvinylidene fluoride (PVDF) membranes (Millipore, IPVH08100). Membranes were blocked in 5 % non-fat milk (Solaribio, D8340) for 2 h, and then incubated with primary antibodies at 4 °C overnight. The following morning, the membranes were washed three times with 0.1 % TBST and then incubated with an appropriate secondary antibody. Signals were detected using a Bio-RAD imaging system. The following primary antibodies were used: MYOC (SC-515500, Santa Cruz Biotechnology), GAPDH (SC-47724, Santa Cruz Biotechnology). HRP-linked anti-mouse IgG (Cell Signaling, 7076) was used as the secondary antibody.

2.11. Statistical analysis

Statistical data are reported as the mean ± standard error. Statistical analysis was performed using GraphPad Prism software. Student's unpaired t-tests were used to compare data between two groups, and one-way analysis of variance was used for comparisons between more than two groups. $P < 0.05$ was considered to indicate a statistically significant difference.

3. Results

3.1. TM cells that overexpressed MYOC^{S341P} were more sensitive to mechanical stress

First, we characterized the specific origin of human primary TM cells by Dex treatment. We observed the robust expression of MYOC protein following Dex treatment (Fig. 1A and B). Next, we investigated the ability of MYOC^{S341P} to cope with mechanical stress by overexpressing MYOC^{S341P} in TM cells and then applying CMS. As shown in Fig. 1C–E, the levels of MYOC mRNA (Fig. 1C) and protein (Fig. 1D and E) MYOC were both significantly upregulated. The overexpression of MYOC^{S341P} in TM cells by lentiviral infection without CMS is depicted in Fig. S1. Next, we performed flow cytometry and found that cell death increased after CMS; Furthermore, TM cells that overexpressed MYOC^{S341P} were more sensitive to CMS, as indicated by a far greater increase in cell death than normal TM cells (Fig. 1F and G).

3.2. DEGs in TM cells under CMS

Next, we investigated the genetic changes of TM cells that overexpressed MYOC^{S341P} in response to CMS, TM cells that had been transfected with the empty vector and TM cells that overexpressed MYOC^{S341P} were subjected to CMS at 20 % stretch, 1 Hz, for 24 h. Cells in the control group were cultured under the same conditions, except that they did not undergo CMS. After RNA sequencing, we identified DEGs using the following criteria: (i) fold change $\geq$1.5 or $\leq$0.66; and (ii) $P < 0.05$.

Fig. 2A shows a heatmap of gene expression in TM cells transfected with the empty vector (defined as TM) and TM cells transfected with the empty vector and treated by CMS (defined as TM-CMS). A total of 1159 DEGs were identified; of these, 316 were upregulated and 843 were downregulated (Fig. 2A). Fig. 2B and C shows a heatmap of the top 20 upregulated and downregulated genes. The gene showing the greatest upregulation in response to mechanical stimulation was CYP1A1; this gene encodes a member of the cytochrome P450 superfamily of enzymes and plays a critical role in the biotransformation and detoxification of xenobiotics [16]. This finding indicated that CMS caused harmful stress when applied to the TM cells. The gene most strongly downregulated in response to mechanical stimulation was TGFA. TGFA is a mitogenic polypeptide with a high affinity for the epidermal growth factor receptor. Reduced TGFA expression has been correlated with the inhibition of cell proliferation [17]; thus, this result implies that the proliferation of TM cells was inhibited by CMS.

A total of 271 DEGs were identified between the TM-CMS and TM cells that overexpressed MYOC^{S341P} and were treated by CMS (defined as the S341P-CMS group); of these, 233 were upregulated and 38 were downregulated (Fig. 2D). A heatmap of the top 20 upregulated and downregulated genes is shown in Fig. 2E and F. The most strongly upregulated gene in the S341P-CMS group was CHRNA3, which encodes a member of the nicotinic acetylcholine receptor family of proteins. Polymorphisms in CHRNA3 have been reported to increase the risk of smoking initiation and susceptibility to lung cancer [18]. The most downregulated gene was RIT2; It

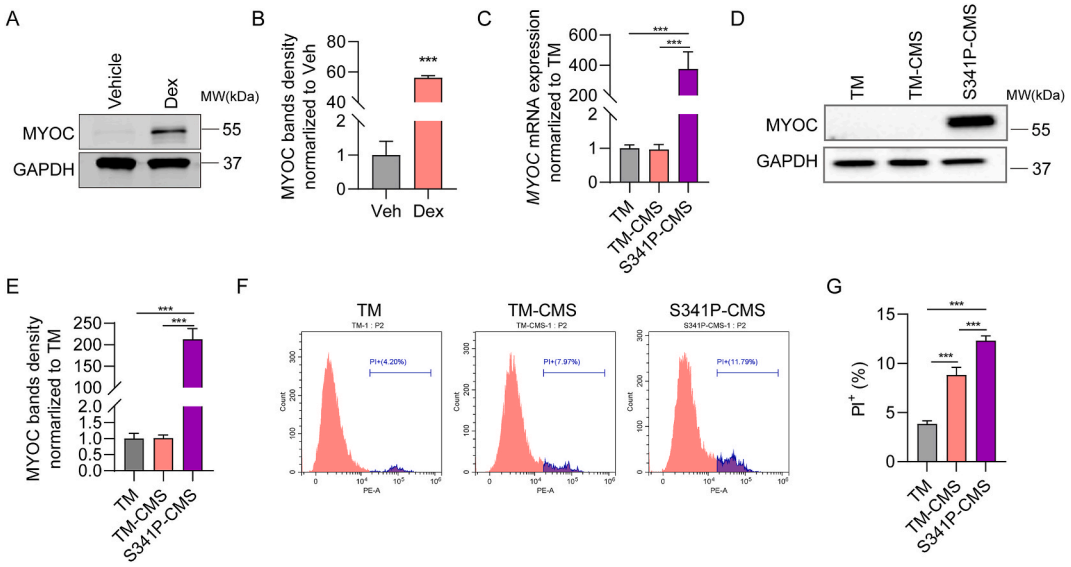

Fig. 1. The detection of cell death in human trabecular meshwork (TM) cells after cyclic mechanical stretch (CMS). (A) Western blot detection of MYOC and GAPDH protein expression in TM cells with and without Dex treatment. (B) MYOC band intensity normalized to that of the untreated group, as determined by ImageJ software. ***$P < 0.001$. (C) qPCR analysis of MYOC mRNA expression in the TM, TM-CMS and S341P-CMS groups. ***$P < 0.001$. (D) Western blot detection of MYOC and GAPDH protein expression in the TM, TM-CMS and S341P-CMS groups. (E) MYOC band intensity normalized to that of the TM group, as determined by ImageJ software (right). ***$P < 0.001$. (F, G) Flow cytometry analysis (F) and statistical analysis (G) of TM cells without CMS, and in the TM-CMS and S341P-CMS groups. All the full, non-adjusted images of Western blot are provided in Fig. S2. ***$P < 0.001$.

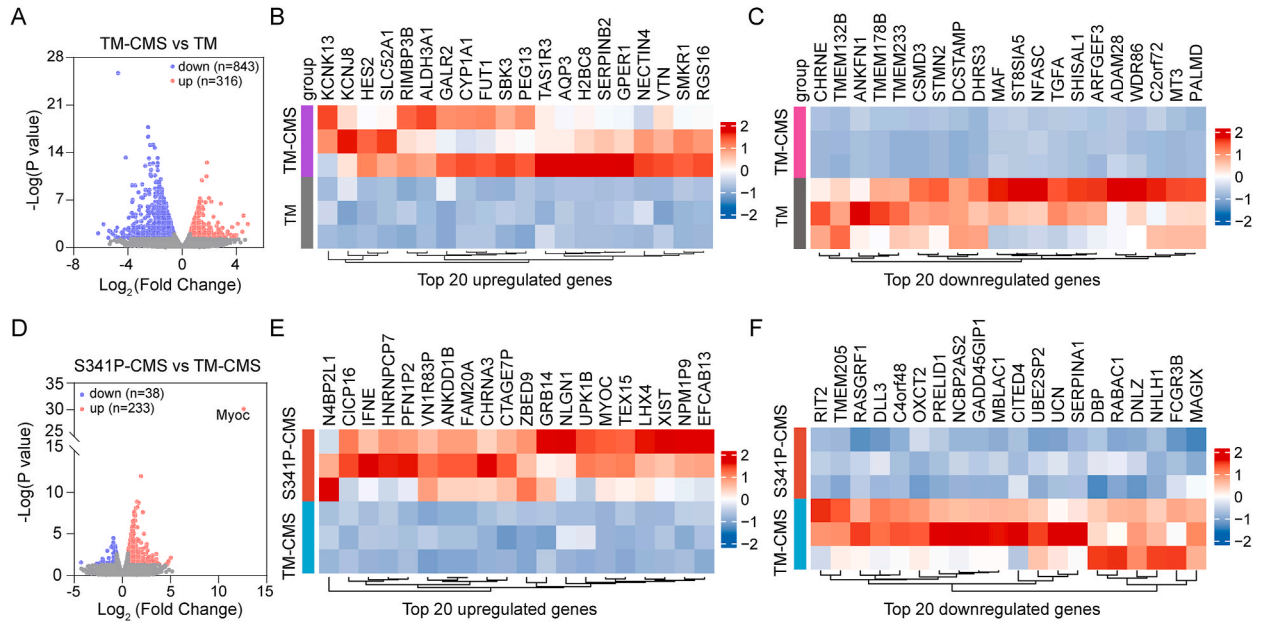

Fig. 2. DEG analysis arising from transcriptomic data. (A) Volcano plot analysis of genes that were markedly regulated by CMS. (B) Heatmap showing the abundance of the top 20 upregulated transcripts when compared between the TM and TM-CMS groups. (C) Heatmap showing the abundance of the top 20 downregulated transcripts when compared between the TM and TM-CMS groups. (D) Volcano plot analysis of genes that were significantly regulated when compared between the S341P-CMS and TM-CMS groups. (E) Heatmap showing the abundance of the top 20 upregulated transcripts when compared between the S341P-CMS and TM-CMS group. (F) Heatmaps showing the abundance of the top 20 downregulated transcripts when compared between the S341P-CMS and TM-CMS groups.

belongs to the RAS superfamily of small GTPases and plays a key role in calcium signaling [19,20]. Calcium oscillations are closely associated with pressure perception and regulation in TM cells [21], thus implying that calcium signaling may have been dysfunctional in the S341P-CMS group.

3.3. Gene ontology (GO) and KEGG analyses of DEGs in TM cells subjected to CMS

Next, we performed GO analysis with the DEGs and found that CMS induced marked upregulation of genes related to lipid response, the negative regulation of cell proliferation, and oxidoreductase activity (Fig. 3A), and significant downregulation of genes involved in extracellular matrix organization, collagen-containing extracellular matrix, and extracellular matrix (Fig. 3B). Thus, we hypothesized that CMS induces an imbalance in the redox microenvironment and abnormal extracellular matrix organization. Notably, in the S341P-CMS group, CMS upregulated genes associated with the cell cycle and double-strand break repair (Fig. 3C), and downregulated genes involved in positive regulation of cellular respiration, negative regulation of cytochrome *c* release, and negative control of necrotic cell death (Fig. 3D). Therefore, we propose that $MYOC^{S341P}$ aggravates damage to TM cells via mitochondria-related pathways.

In addition to GO analysis, we used KEGG pathway enrichment analysis to investigate how S341P influenced the response to CMS stimulation. Following CMS, alterations were detected in signaling pathways associated with mitophagy, autophagy, necroptosis, cell adhesion, and extracellular matrix (ECM)–receptor interaction in the TM-CMS group (Fig. 4A). In the 341P-CMS group, we identified enrichment in mitophagy, autophagy, and signaling pathways associated with homologous recombination, ubiquitin-mediated proteolysis, and RAS signaling (Fig. 4B). Furthermore, gene set enrichment analysis (GSEA) showed that mitochondrial function was impaired in the S341P-CMS group, as evidenced by the downregulation of oxidative phosphorylation and respiratory electron transport signaling (Fig. 4C and D). Based on enrichment score (ES), the top five genes in oxidative phosphorylation pathway were *ATP5ME*, *NDUFV3*, *MT-CO3*, *ATP6V1H* and *ATP6V1D*, while the top five genes in respiratory electron transport pathway were *NDUFV3*, *NDUFAF1*, *CYCS*, *SDHC*, and *NDUFAF5*. The downwards trend in the expression of these genes may lead to mitochondrial dysfunction, thereby increasing sensitivity to CMS.

3.4. Validation of DEGs by qPCR

Next, we investigated gene expression patterns to identify genes associated with aggravated injury in the S341P-CMS group. The resulting heatmap revealed different gene expression patterns between the TM and TM-CMS groups, and between the S341P-CMS and TM-CMS groups (Fig. 5A). We selected genes with much lower expression levels or much higher expression levels (a fold change $\geq$1.5 or $\leq$0.66) in the S341P-CMS group when compared with the TM and TM-CMS groups (Fig. 5B). Four genes were identified (SARM1, AHNAK2, NT5C, and SOX8) and subsequently confirmed by qPCR analysis. Following CMS, the mRNA levels of SARM1, AHNAK2 and

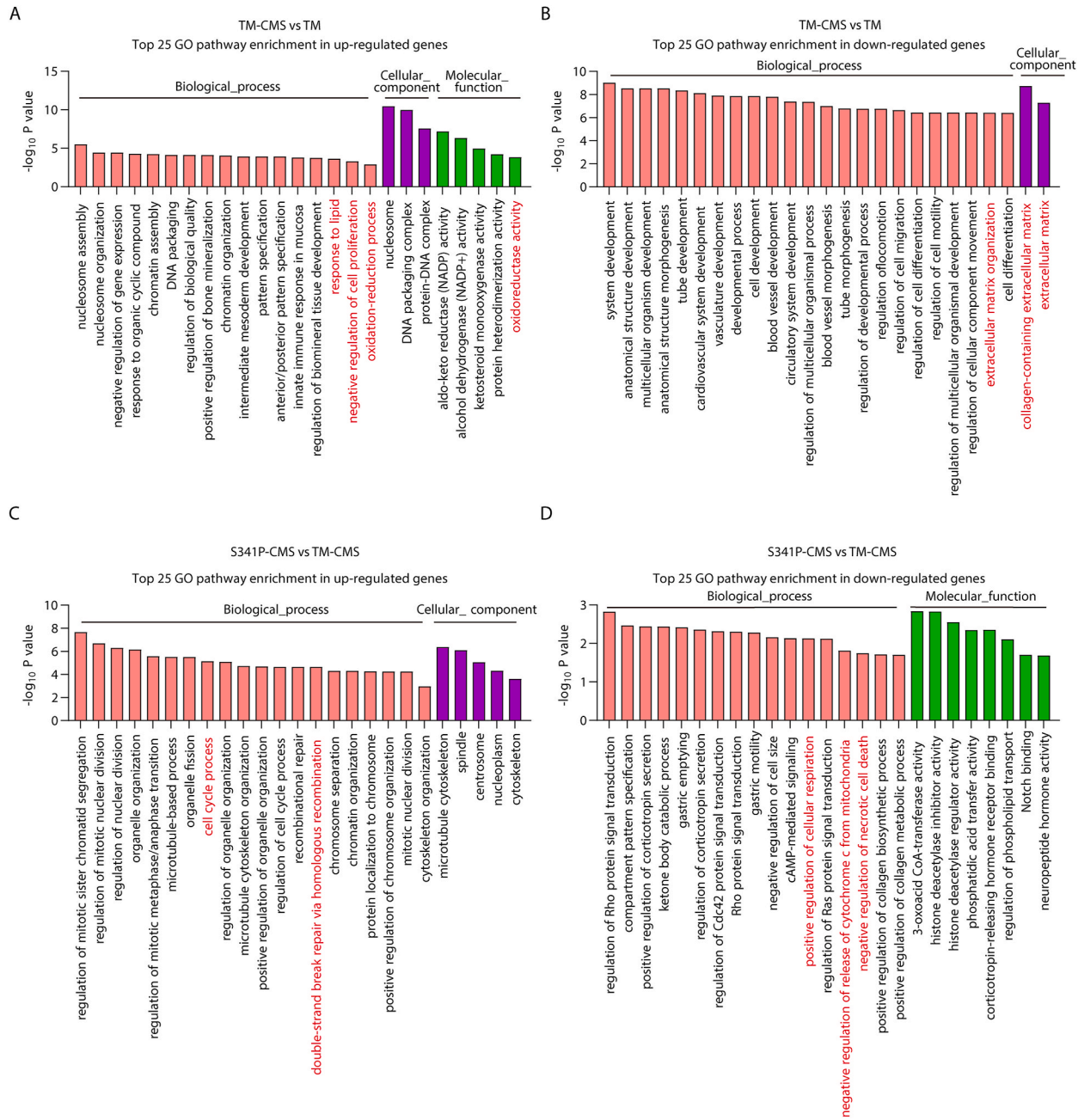

Fig. 3. GO analysis of DEGs. (A) GO analysis of upregulated genes between the TM-CMS and TM groups. (B) GO analysis of downregulated genes between the TM-CMS and TM groups. (C) GO analysis of upregulated genes between the S341P-CMS and TM-CMS groups. (D) GO analysis of downregulated genes between the S341P-CMS and TM-CMS groups.

NT5C were increased in TM cells, with much higher levels in the S341P-CMS group (Fig. 5C). In contrast, the mRNA levels of SOX8 decreased after CMS; furthermore, the expression levels of this gene were much lower in the S341P-CMS group (Fig. 5C). According to GSEA, mitochondrial function was dysregulated in the S341P-CMS group. Mitochondria are a source of reactive oxygen species (ROS), which are strong associated with oxidative stress [22]. We also performed oxidized lipidomics to analyze the oxylipin levels; the results of this analysis are shown as heatmaps in Fig. 6A and B. We observed marked changes in the oxylipin profile when compared between the three groups, including arachidonic acid (Fig. 6A) and docosahexaenoic acid (Fig. 6B). Arachidonic acid (ARA) is an essential component of mammalian cell membrane phospholipids and generates various oxylipins via the cyclooxygenase (COX), lipoxygenase (LOX), and cytochrome P450 (CYP) pathways, including prostaglandins (PGEs), leukotrienes, and epoxy metabolites. These oxylipins can influence mitochondrial function by increasing the production of mitochondrial ROS and by influencing calcium homeostasis [23,

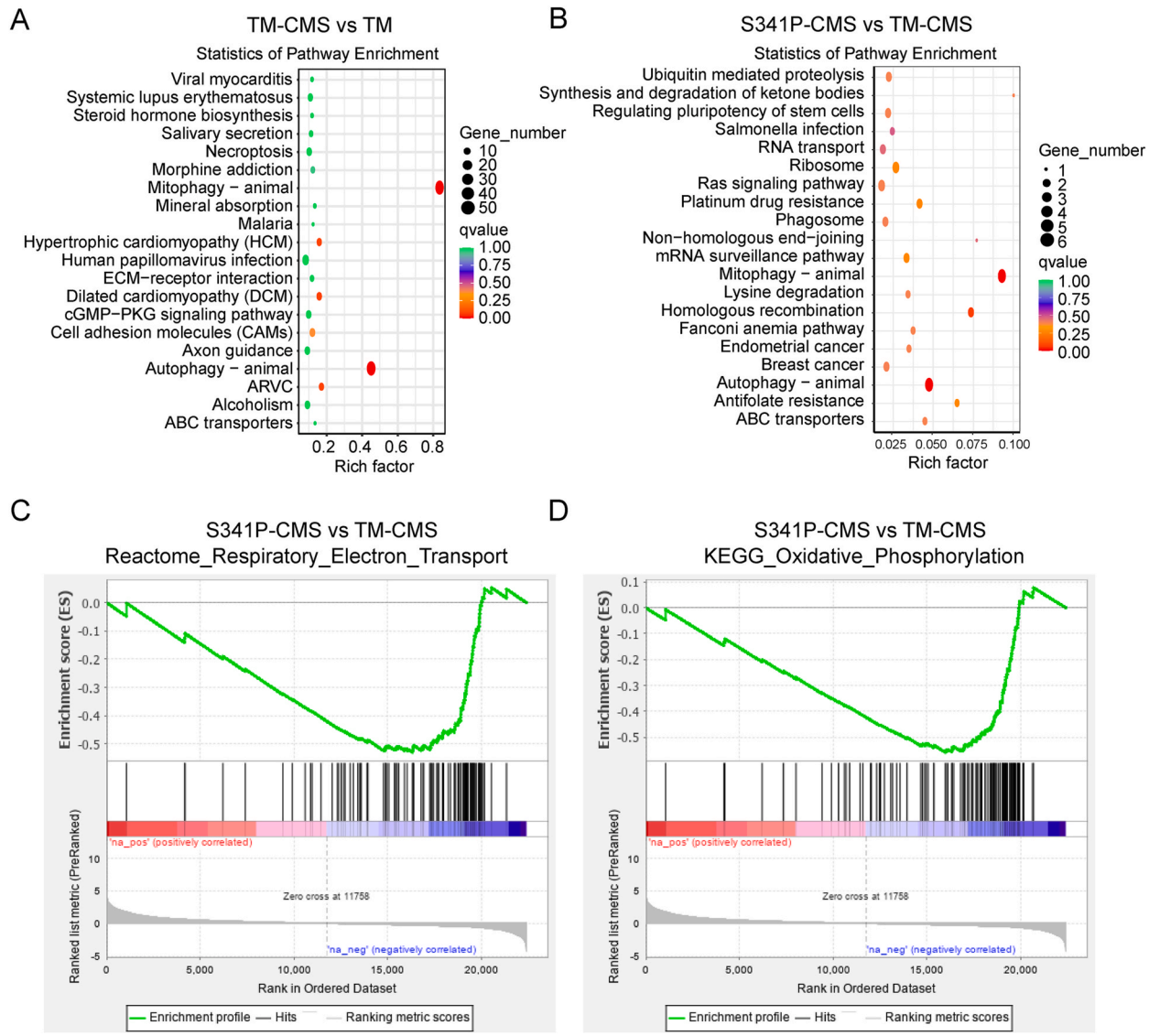

Fig. 4. KEGG and GSEA analyses of DEGs. (A) KEGG pathway enrichment analysis between the TM-CMS and TM group. (B) KEGG pathway enrichment analysis between the S341P-CMS and TM-CMS groups. (C, D) GSEA analysis between the S341P-CMS and TM-CMS group.

24]. Docosahexaenoic acid (DHA) is a highly abundant polyunsaturated fatty acid (PUFA) in the brain and retina, and produces various oxylipins via similar enzymatic pathways. DHA plays a crucial role in maintaining mitochondrial function and cell survival [25]. Oxylipins of DHA may also contribute to mitochondria dysfunction. Collectively, these results suggest that the increased sensitivity to CMS in TM cells that overexpressed MYOC^{S341P} may be related to mitochondrial dysfunction caused by alterations in genes associated with mitochondrial function and lipid metabolism, as identified by GSEA. These results indicate that the increased sensitivity to CMS in TM cells that overexpressed MYOC^{S341P} may be associated with mitochondrial dysfunction.

4. Discussion

TM tissue has evolved to adapt to CMS stimulation to maintain homeostasis in the outflow of aqueous humor [26]. However, patients with glaucoma exhibit different biomechanics in the TM tissues when compared with age-matched healthy controls [27]. To better understand the biomechanical properties of TM cells under CMS with or without the overexpression of MYOC^{S341P}, we systematically identified and validated DEGs between TM and TM-CMS groups and between S341P-CMS and TM-CMS groups. In particular, we found that mitochondrial dysfunction may be involved in the TM damage induced by MYOC^{S341P}.

Generally, TM cells adjust to mechanical stress by activating downstream signaling pathways [28]. The adaptive mechanism includes, but is not limited to, integrin signaling [29], cationic mechanosensitive channels mediating changes in the composition of the

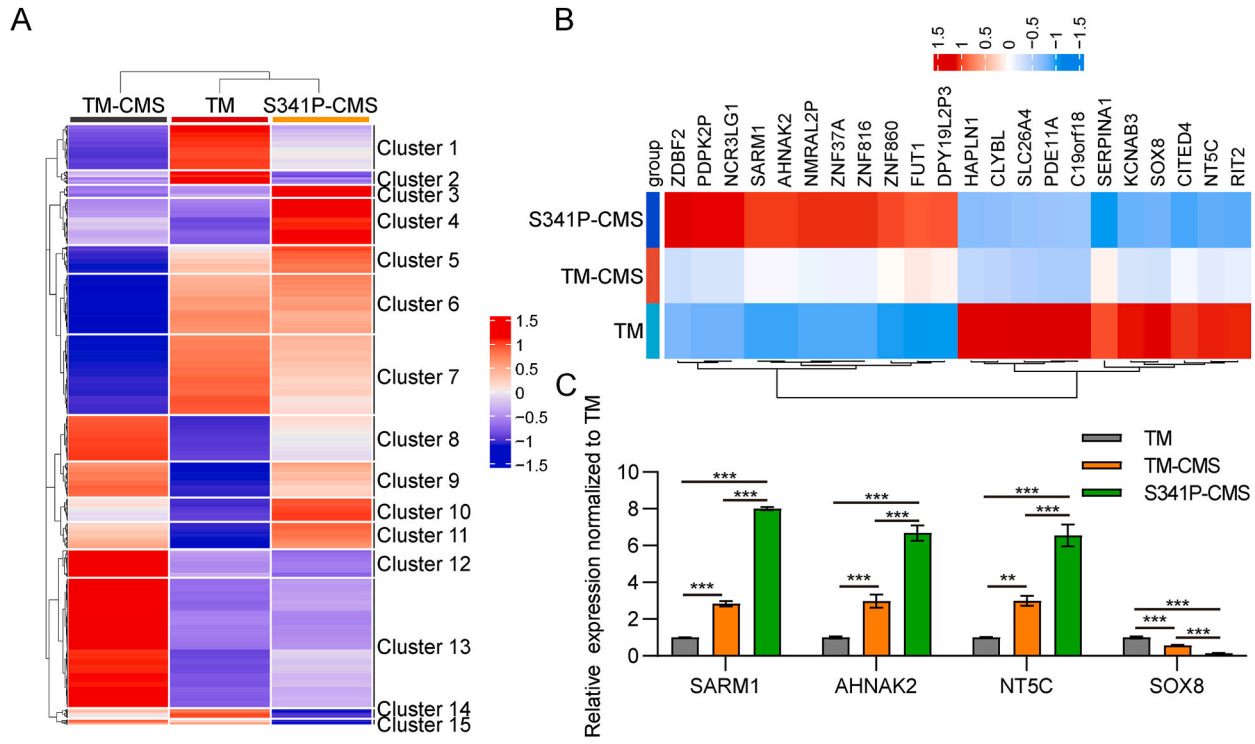

Fig. 5. Expression pattern analysis of DEGs. (A) Heatmaps showing gene expression patterns in the TM, TM-CMS, and S341P-CMS groups. (B) Heatmaps of DEGs between the TM, TM-CMS, and S341P-CMS groups. (C) qPCR analysis of SARM1, AHNAK2, NT5C and SOX8 mRNA expression levels in the TM, TM-CMS, and S341P-CMS groups. *P < 0.05, **P < 0.01, ***P < 0.001.

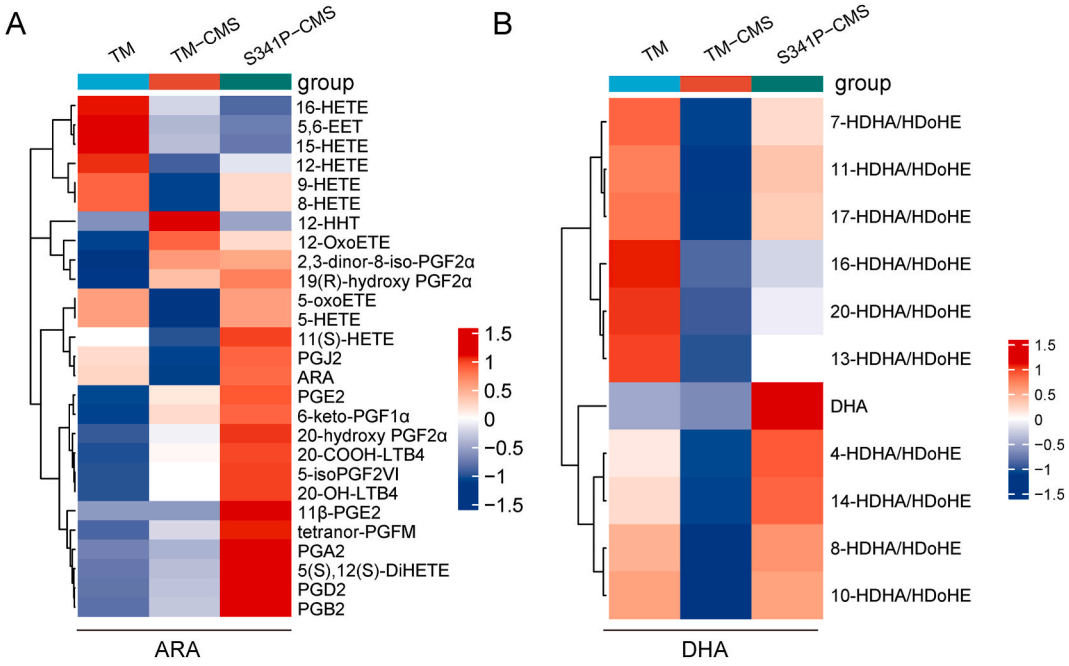

Fig. 6. Oxylipin profiles under CMS. (A) Heatmap showing differences in the arachidonic acid (ARA) content between the TM, TM-CMS, and S341P-CMS groups. (B) Heatmap showing differences in docosahexaenoic acid (DHA) content between the TM, TM-CMS, and S341P-CMS groups.

extracellular matrix (ECM) and cytoskeleton remodeling [5], and autophagy [30]. Following CMS, we consistently identified changes in the biological processes associated with ECM organization. Furthermore, we found that CMS led to alterations in oxidoreductase activity, indicating impaired redox homeostasis following mechanical stretch. Thus, protective signaling occurs in the TM to counter mechanical stretch and maintain homeostasis. However, there are also negative signaling pathways that can impair TM cells, including necroptosis. Therefore, the balance between protective signaling and injury-related signaling is crucial for TM cells.

The aggregation of mutant MYOC due to impaired autophagy is known to cause damage to TM cells without mechanical stress, as reported previously [13,31]. Under the conditions of mechanical stretch, we found that TM cells that overexpressed $MYOC^{S341P}$ were more sensitive to CMS. We hypothesized that activated autophagy in mechanically stretched TM cells could have partially compromised the dysregulated autophagy in the $MYOC^{S341P}$ group, and that the upregulated autophagy eventually led to over-activated autophagy. It has been reported that the hyper-activation of autophagy can be harmful to the retina, and that the inhibition of autophagy can protect the retina from light injury [32]. Other studies have supported the concept of autophagy as a double-edged sword [33,34]. Further studies are now needed to confirm that the over-activation of autophagy in $MYOC^{S341P}$ cells following CMS stimulation can impair the functionality of TM cells. In addition to autophagy, we also observed changes in signaling pathways associated with homologous recombination, ubiquitin-mediated proteolysis, and RAS signaling in TM cells that overexpressed $MYOC^{S341P}$.

In the present study, we performed oxylipin profiling to investigate the metabolic changes associated with $MYOC^{S341P}$ overexpression in TM cells under CMS. Our profiling identified several key oxylipins derived from ARA, which were significantly altered in the TM-S341P-CMS group. We observed a significant increase in prostaglandin E2 (PGE2) and leukotriene B4 (LTB4) levels. PGE2 is known to affect mitochondrial membrane potential [35], while LTB4 can increase mitochondrial ROS production [36], leading to oxidative stress and mitochondrial damage. Oxylipins are bioactive lipids that play crucial roles in inflammation, oxidative stress, and cell death; all of these processes are intimately linked to mitochondrial function. By profiling these molecules, we aimed to identify the metabolic pathways affected by $MYOC^{S341P}$ overexpression and their potential contributions to dysfunction in TM cells.

We also observed differential expression patterns between the TM and TM-CMS groups, and between the S341P-CMS and TM-CMS groups, and identified four genes which underwent expression changes in TM cells that overexpressed $MYOC^{S341P}$ under CMS. Notably, these genes included SARM1 and SOX8. SARM1, a NAD + hydrolase that is associated with cell death in response to injury or stress [37]. This could explain the increased rate of cell death in the S341P-CMS group when compared with the TM-CMS group. The downregulation of SOX8 has been reported to impair autophagy. The much lower expression levels of SOX8 in the S341P-CMS group may have exacerbated autophagy impairment, further damaging TM cells.

In summary, this study identified the main mechanism underlying damage to TM cells with $MYOC^{S341P}$ overexpression under CMS. Regulation of mitochondrial function may provide a potential treatment direction for patients with primary open-angle glaucoma carrying MYOC mutations.

Funding statement

This study was supported by National Natural Science Foundation of China (82301195, 82130029), Beijing Natural Science Foundation (L212036), Beijing Municipal Public Welfare Development and Reform Pilot Project for Medical Research Institutes (PWD&RPP-MRI, JYY2023-6).

Data availability statement

The datasets used and analyzed during the current study are available from the corresponding author on reasonable request.

CRediT authorship contribution statement

Xuejing Yan: Writing – review & editing, Writing – original draft, Validation, Methodology, Funding acquisition, Formal analysis, Conceptualization. **Shen Wu:** Writing – review & editing, Methodology. **Qian Liu:** Writing – review & editing, Methodology. **Yufei Teng:** Writing – review & editing, Methodology. **Ningli Wang:** Writing – review & editing, Investigation, Funding acquisition. **Jingxue Zhang:** Writing – review & editing, Methodology, Funding acquisition, Conceptualization.

Declaration of competing interest

The authors declare that they have no known competing financial interests or personal relationships that could have appeared to influence the work reported in this paper.

Appendix A. Supplementary data

Supplementary data to this article can be found online at https://doi.org/10.1016/j.heliyon.2024.e37137.

References

[1] G.B.D. Blindness, C. Vision Impairment, Vision Loss Expert Group of the Global Burden of Disease S, Causes of blindness and vision impairment in 2020 and trends over 30 years, and prevalence of avoidable blindness in relation to VISION 2020: the Right to Sight: an analysis for the Global Burden of Disease Study, Lancet Global Health 9 (2) (2021) e144–e160.

[2] Y.C. Tham, X. Li, T.Y. Wong, H.A. Quigley, T. Aung, C.Y. Cheng, Global prevalence of glaucoma and projections of glaucoma burden through 2040: a systematic review and meta-analysis, Ophthalmology 121 (11) (2014) 2081–2090.

[3] J. Hirt, P.B. Liton, Autophagy and mechanotransduction in outflow pathway cells, Exp. Eye Res. 158 (2017) 146–153.

[4] H. Youngblood, J. Cai, M.D. Drewry, I. Helwa, E. Hu, S. Liu, et al., Expression of mRNAs, miRNAs, and lncRNAs in human trabecular meshwork cells upon mechanical stretch, Invest. Ophthalmol. Vis. Sci. 61 (5) (2020) 2.

[5] S. Chen, W. Wang, Q. Cao, S. Wu, N. Wang, L. Ji, et al., Cationic mechanosensitive channels mediate trabecular meshwork responses to cyclic mechanical stretch, Front. Pharmacol. 13 (2022) 881286.

[6] K.E. Keller, M.J. Kelley, T.S. Acott, Extracellular matrix gene alternative splicing by trabecular meshwork cells in response to mechanical stretching, Invest. Ophthalmol. Vis. Sci. 48 (3) (2007) 1164–1172.

[7] E. Reina-Torres, M.L. De Ieso, L.R. Pasquale, M. Madekurozwa, J. van Batenburg-Sherwood, D.R. Overby, et al., The vital role for nitric oxide in intraocular pressure homeostasis, Prog. Retin. Eye Res. 83 (2021) 100922.

[8] M.S. Shim, A. Nettesheim, J. Hirt, P.B. Liton, The autophagic protein LC3 translocates to the nucleus and localizes in the nucleolus associated to NUFIP1 in response to cyclic mechanical stress, Autophagy 16 (7) (2020) 1248–1261.

[9] E.M. Stone, J.H. Fingert, W.L. Alward, T.D. Nguyen, J.R. Polansky, S.L. Sunden, et al., Identification of a gene that causes primary open angle glaucoma, Science 275 (5300) (1997) 668–670.

[10] F. Wang, Y. Li, L. Lan, B. Li, L. Lin, X. Lu, et al., Ser341Pro MYOC gene mutation in a family with primary open-angle glaucoma, Int. J. Mol. Med. 35 (5) (2015) 1230–1236.

[11] X. Yan, S. Wu, Q. Liu, Y. Li, W. Zhu, J. Zhang, Accumulation of Asn450Tyr mutant myocilin in ER promotes apoptosis of human trabecular meshwork cells, Mol. Vis. 26 (2020) 563–573.

[12] R.B. Kasetti, P. Maddineni, C. Kiehlbauch, S. Patil, C.C. Searby, B. Levine, et al., Autophagy stimulation reduces ocular hypertension in a murine glaucoma model via autophagic degradation of mutant myocilin, JCI Insight 6 (5) (2021) e143359.

[13] X. Yan, S. Wu, Q. Liu, Y. Cheng, J. Zhang, N. Wang, Myocilin gene mutation induced autophagy activation causes dysfunction of trabecular meshwork cells, Front. Cell Dev. Biol. 10 (2022) 900777.

[14] B.M. Welch, E.E. McNell, M.L. Edin, K.K. Ferguson, Inflammation and oxidative stress as mediators of the impacts of environmental exposures on human pregnancy: evidence from oxylipins, Pharmacol. Ther. 239 (2022) 108181.

[15] J. Xu, C. Fu, Y. Sun, X. Wen, C.B. Chen, C. Huang, et al., Untargeted and oxylipin-targeted metabolomics study on the plasma samples of primary open-angle glaucoma patients, Biomolecules 14 (3) (2024) 307.

[16] M. Kyoreva, Y. Li, M. Hoosenally, J. Hardman-Smart, K. Morrison, I. Tosi, et al., CYP1A1 enzymatic activity influences skin inflammation via regulation of the AHR pathway, J. Invest. Dermatol. 141 (6) (2021) 1553–15563 e3.

[17] X. Ma, J. Zheng, K. He, L. Wang, Z. Wang, K. Wang, et al., TGFA expression is associated with poor prognosis and promotes the development of cervical cancer, J. Cell Mol. Med. 28 (3) (2024) e18086.

[18] R. Perez-Morales, A. Gonzalez-Zamora, M.F. Gonzalez-Delgado, E.Y. Calleros Rincon, E.H. Olivas Calderon, O.C. Martinez-Ramirez, et al., CHRNA3 rs1051730 and CHRNA5 rs16969968 polymorphisms are associated with heavy smoking, lung cancer, and chronic obstructive pulmonary disease in a mexican population, Ann. Hum. Genet. 82 (6) (2018) 415–424.

[19] C.H. Lee, N.G. Della, C.E. Chew, D.J. Zack, Rin, a neuron-specific and calmodulin-binding small G-protein, and Rit define a novel subfamily of ras proteins, J. Neurosci. 16 (21) (1996) 6784–6794.

[20] M. Hoshino, S. Nakamura, Small GTPase Rin induces neurite outgrowth through Rac/Cdc42 and calmodulin in PC12 cells, J. Cell Biol. 163 (5) (2003) 1067–1076.

[21] O. Yarishkin, T.T.T. Phuong, F. Vazquez-Chona, J. Bertrand, J. van Battenburg-Sherwood, S.N. Redmon, et al., Emergent temporal signaling in human trabecular meshwork cells: role of TRPV4-TRPM4 interactions, Front. Immunol. 13 (2022) 805076.

[22] N.D. Magnani, T. Marchini, V. Calabro, S. Alvarez, P. Evelson, Role of mitochondria in the redox signaling network and its outcomes in high impact inflammatory syndromes, Front. Endocrinol. 11 (2020) 568305.

[23] Y. Izquierdo, L. Muniz, J. Vicente, S. Kulasekaran, V. Aguilera, A. Lopez Sanchez, et al., Oxylipins from different pathways trigger mitochondrial stress signaling through respiratory complex III, Front. Plant Sci. 12 (2021) 705373.

[24] V. Barquissau, R.A. Ghandour, G. Ailhaud, M. Klingenspor, D. Langin, E.Z. Amri, et al., Control of adipogenesis by oxylipins, GPCRs and PPARs, Biochimie 136 (2017) 3–11.

[25] G. Li, Y. Li, B. Xiao, D. Cui, Y. Lin, J. Zeng, et al., Antioxidant activity of docosahexaenoic acid (DHA) and its regulatory roles in mitochondria, J. Agric. Food Chem. 69 (5) (2021) 1647–1655.

[26] D.C. Turner, A.M. Edmiston, Y.E. Zohner, K.J. Byrne, W.P. Seigfreid, C.A. Girkin, et al., Transient intraocular pressure fluctuations: source, magnitude, frequency, and associated mechanical energy, Invest. Ophthalmol. Vis. Sci. 60 (7) (2019) 2572–2582.

[27] V.K. Raghunathan, J. Benoit, R. Kasetti, G. Zode, M. Salemi, B.S. Phinney, et al., Glaucomatous cell derived matrices differentially modulate non-glaucomatous trabecular meshwork cellular behavior, Acta Biomater. 71 (2018) 444–459.

[28] T.S. Acott, J.A. Vranka, K.E. Keller, V. Raghunathan, M.J. Kelley, Normal and glaucomatous outflow regulation, Prog. Retin. Eye Res. 82 (2021) 100897.

[29] Y.F. Yang, Y.Y. Sun, D.M. Peters, K.E. Keller, The effects of mechanical stretch on integrins and filopodial-associated proteins in normal and glaucomatous trabecular meshwork cells, Front. Cell Dev. Biol. 10 (2022) 886706.

[30] M.S. Shim, A. Nettesheim, A. Dixon, P.B. Liton, Primary cilia and the reciprocal activation of AKT and SMAD2/3 regulate stretch-induced autophagy in trabecular meshwork cells, Proc. Natl. Acad. Sci. U.S.A. 118 (13) (2021) e2021942118.

[31] K. Porter, J. Hirt, W.D. Stamer, P.B. Liton, Autophagic dysregulation in glaucomatous trabecular meshwork cells, Biochim. Biophys. Acta 1852 (3) (2015) 379–385.

[32] J. Song, Y. Liu, T. Wang, B. Li, S. Zhang, MiR-17-5p promotes cellular proliferation and invasiveness by targeting RUNX3 in gastric cancer, Biomed. Pharmacother. 128 (2020) 110246.

[33] D. Xu, T. Kong, S. Zhang, B. Cheng, J. Chen, C. Wang, Orexin-A protects against cerebral ischemia-reperfusion injury by inhibiting excessive autophagy through OX1R-mediated MAPK/ERK/mTOR pathway, Cell. Signal. 79 (2021) 109839.

[34] L. Chen, Z. Lv, Z. Gao, G. Ge, X. Wang, J. Zhou, et al., Human beta-defensin-3 reduces excessive autophagy in intestinal epithelial cells and in experimental necrotizing enterocolitis, Sci. Rep. 9 (1) (2019) 19890.

[35] D.E. Sanin, M. Matsushita, R.I. Klein Geltink, K.M. Grzes, N. van Teijlingen Bakker, M. Corrado, et al., Mitochondrial membrane potential regulates nuclear gene expression in macrophages exposed to prostaglandin E2, Immunity 49 (6) (2018) 1021–10233 e6.

[36] P. Barcellos-de-Souza, C. Canetti, C. Barja-Fidalgo, M.A. Arruda, Leukotriene B(4) inhibits neutrophil apoptosis via NADPH oxidase activity: redox control of NF-kappaB pathway and mitochondrial stability, Biochim. Biophys. Acta 1823 (10) (2012) 1990–1997.

[37] J. Peng, Q. Yuan, B. Lin, P. Panneerselvam, X. Wang, X.L. Luan, et al., SARM inhibits both TRIF- and MyD88-mediated AP-1 activation, Eur. J. Immunol. 40 (6) (2010) 1738–1747.